

***B* Meson Decays to ωK^* , $\omega\rho$, $\omega\omega$, $\omega\phi$, and ωf_0**

B. Aubert,¹ R. Barate,¹ M. Bona,¹ D. Boutigny,¹ F. Couderc,¹ Y. Karyotakis,¹ J. P. Lees,¹ V. Poireau,¹ V. Tisserand,¹ A. Zghiche,¹ E. Grauges,² A. Palano,³ J. C. Chen,⁴ N. D. Qi,⁴ G. Rong,⁴ P. Wang,⁴ Y. S. Zhu,⁴ G. Eigen,⁵ I. Ofte,⁵ B. Stugu,⁵ G. S. Abrams,⁶ M. Battaglia,⁶ D. N. Brown,⁶ J. Button-Shafer,⁶ R. N. Cahn,⁶ E. Charles,⁶ M. S. Gill,⁶ Y. Groyzman,⁶ R. G. Jacobsen,⁶ J. A. Kadyk,⁶ L. T. Kerth,⁶ Yu. G. Kolomensky,⁶ G. Kukartsev,⁶ G. Lynch,⁶ L. M. Mir,⁶ P. J. Oddone,⁶ T. J. Orimoto,⁶ M. Pripstein,⁶ N. A. Roe,⁶ M. T. Ronan,⁶ W. A. Wenzel,⁶ M. Barrett,⁷ K. E. Ford,⁷ T. J. Harrison,⁷ A. J. Hart,⁷ C. M. Hawkes,⁷ S. E. Morgan,⁷ A. T. Watson,⁷ K. Goetzen,⁸ T. Held,⁸ H. Koch,⁸ B. Lewandowski,⁸ M. Pelizaeus,⁸ K. Peters,⁸ T. Schroeder,⁸ M. Steinke,⁸ J. T. Boyd,⁹ J. P. Burke,⁹ W. N. Cottingham,⁹ D. Walker,⁹ T. Cuhadar-Donszelmann,¹⁰ B. G. Fulsom,¹⁰ C. Hearty,¹⁰ N. S. Knecht,¹⁰ T. S. Mattison,¹⁰ J. A. McKenna,¹⁰ A. Khan,¹¹ P. Kyberd,¹¹ M. Saleem,¹¹ L. Teodorescu,¹¹ V. E. Blinov,¹² A. D. Bukin,¹² V. P. Druzhinin,¹² V. B. Golubev,¹² A. P. Onuchin,¹² S. I. Serednyakov,¹² Yu. I. Skovpen,¹² E. P. Solodov,¹² K. Yu Todyshev,¹² D. S. Best,¹³ M. Bondioli,¹³ M. Bruinsma,¹³ M. Chao,¹³ S. Curry,¹³ I. Eschrich,¹³ D. Kirkby,¹³ A. J. Lankford,¹³ P. Lund,¹³ M. Mandelkern,¹³ R. K. Mommsen,¹³ W. Roethel,¹³ D. P. Stoker,¹³ S. Abachi,¹⁴ C. Buchanan,¹⁴ S. D. Foulkes,¹⁵ J. W. Gary,¹⁵ O. Long,¹⁵ B. C. Shen,¹⁵ K. Wang,¹⁵ L. Zhang,¹⁵ H. K. Hadavand,¹⁶ E. J. Hill,¹⁶ H. P. Paar,¹⁶ S. Rahatlou,¹⁶ V. Sharma,¹⁶ J. W. Berryhill,¹⁷ C. Campagnari,¹⁷ A. Cunha,¹⁷ B. Dahmes,¹⁷ T. M. Hong,¹⁷ D. Kovalskiy,¹⁷ J. D. Richman,¹⁷ T. W. Beck,¹⁸ A. M. Eisner,¹⁸ C. J. Flacco,¹⁸ C. A. Heusch,¹⁸ J. Kroseberg,¹⁸ W. S. Lockman,¹⁸ G. Nesom,¹⁸ T. Schalk,¹⁸ B. A. Schumm,¹⁸ A. Seiden,¹⁸ P. Spradlin,¹⁸ D. C. Williams,¹⁸ M. G. Wilson,¹⁸ J. Albert,¹⁹ E. Chen,¹⁹ D. Doll,¹⁹ A. Dvoretzki,¹⁹ D. G. Hitlin,¹⁹ I. Narsky,¹⁹ T. Piatenko,¹⁹ F. C. Porter,¹⁹ A. Ryd,¹⁹ A. Samuel,¹⁹ R. Andreassen,²⁰ G. Mancinelli,²⁰ B. T. Meadows,²⁰ M. D. Sokoloff,²⁰ F. Blanc,²¹ P. C. Bloom,²¹ S. Chen,²¹ W. T. Ford,²¹ J. F. Hirschauer,²¹ A. Kreisel,²¹ U. Nauenberg,²¹ A. Olivas,²¹ W. O. Ruddick,²¹ J. G. Smith,²¹ K. A. Ulmer,²¹ S. R. Wagner,²¹ J. Zhang,²¹ A. Chen,²² E. A. Eckhart,²² A. Soffer,²² W. H. Toki,²² R. J. Wilson,²² F. Winklmeier,²² Q. Zeng,²² D. D. Altenburg,²³ E. Feltresi,²³ A. Hauke,²³ H. Jasper,²³ B. Spaan,²³ T. Brandt,²⁴ V. Klohe,²⁴ H. M. Lacker,²⁴ W. F. Mader,²⁴ R. Nogowski,²⁴ A. Petzold,²⁴ J. Schubert,²⁴ K. R. Schubert,²⁴ R. Schwierz,²⁴ J. E. Sundermann,²⁴ A. Volk,²⁴ D. Bernard,²⁵ G. R. Bonneaud,²⁵ P. Grenier,²⁵ * E. Latour,²⁵ Ch. Thiebaux,²⁵ M. Verderi,²⁵ D. J. Bard,²⁶ P. J. Clark,²⁶ W. Gradl,²⁶ F. Muheim,²⁶ S. Playfer,²⁶ A. I. Robertson,²⁶ Y. Xie,²⁶ M. Andreotti,²⁷ D. Bettoni,²⁷ C. Bozzi,²⁷ R. Calabrese,²⁷ G. Cibinetto,²⁷ E. Luppi,²⁷ M. Negrini,²⁷ A. Petrella,²⁷ L. Piemontese,²⁷ E. Prencipe,²⁷ F. Anulli,²⁸ R. Baldini-Feroli,²⁸ A. Calcaterra,²⁸ R. de Sangro,²⁸ G. Finocchiaro,²⁸ S. Pacetti,²⁸ P. Patteri,²⁸ I. M. Peruzzi,²⁸ † M. Piccolo,²⁸ M. Rama,²⁸ A. Zallo,²⁸ A. Buzzo,²⁹ R. Capra,²⁹ R. Contri,²⁹ M. Lo Vetere,²⁹ M. M. Macri,²⁹ M. R. Monge,²⁹ S. Passaggio,²⁹ C. Patrignani,²⁹ E. Robutti,²⁹ A. Santroni,²⁹ S. Tosi,²⁹ G. Brandenburg,³⁰ K. S. Chaisanguanthum,³⁰ M. Morii,³⁰ J. Wu,³⁰ R. S. Dubitzky,³¹ J. Marks,³¹ S. Schenk,³¹ U. Uwer,³¹ W. Bhimji,³² D. A. Bowerman,³² P. D. Dauncey,³² U. Egede,³² R. L. Flack,³² J. R. Gaillard,³² J. A. Nash,³² M. B. Nikolich,³² W. Panduro Vazquez,³² X. Chai,³³ M. J. Charles,³³ U. Mallik,³³ N. T. Meyer,³³ V. Ziegler,³³ J. Cochran,³⁴ H. B. Crawley,³⁴ L. Dong,³⁴ V. Eyges,³⁴ W. T. Meyer,³⁴ S. Prell,³⁴ E. I. Rosenberg,³⁴ A. E. Rubin,³⁴ A. V. Gritsan,³⁵ M. Fritsch,³⁶ G. Schott,³⁶ N. Arnaud,³⁷ M. Davier,³⁷ G. Grosdidier,³⁷ A. Höcker,³⁷ F. Le Diberder,³⁷ V. Lepeltier,³⁷ A. M. Lutz,³⁷ A. Oyanguren,³⁷ S. Pruvot,³⁷ S. Rodier,³⁷ P. Roudeau,³⁷ M. H. Schune,³⁷ A. Stocchi,³⁷ W. F. Wang,³⁷ G. Wormser,³⁷ C. H. Cheng,³⁸ D. J. Lange,³⁸ D. M. Wright,³⁸ C. A. Chavez,³⁹ I. J. Forster,³⁹ J. R. Fry,³⁹ E. Gabathuler,³⁹ R. Gamet,³⁹ K. A. George,³⁹ D. E. Hutchcroft,³⁹ D. J. Payne,³⁹ K. C. Schofield,³⁹ C. Touramanis,³⁹ A. J. Bevan,⁴⁰ F. Di Lodovico,⁴⁰ W. Menges,⁴⁰ R. Sacco,⁴⁰ C. L. Brown,⁴¹ G. Cowan,⁴¹ H. U. Flaecher,⁴¹ D. A. Hopkins,⁴¹ P. S. Jackson,⁴¹ T. R. McMahon,⁴¹ S. Ricciardi,⁴¹ F. Salvatore,⁴¹ D. N. Brown,⁴² C. L. Davis,⁴² J. Allison,⁴³ N. R. Barlow,⁴³ R. J. Barlow,⁴³ Y. M. Chia,⁴³ C. L. Edgar,⁴³ M. P. Kelly,⁴³ G. D. Lafferty,⁴³ M. T. Naisbit,⁴³ J. C. Williams,⁴³ J. I. Yi,⁴³ C. Chen,⁴⁴ W. D. Hulsbergen,⁴⁴ A. Jawahery,⁴⁴ C. K. Lae,⁴⁴ D. A. Roberts,⁴⁴ G. Simi,⁴⁴ G. Blaylock,⁴⁵ C. Dallapiccola,⁴⁵ S. S. Hertzbach,⁴⁵ X. Li,⁴⁵ T. B. Moore,⁴⁵ S. Saremi,⁴⁵ H. Staengle,⁴⁵ S. Y. Willocq,⁴⁵ R. Cowan,⁴⁶ K. Koeneke,⁴⁶ G. Sciolla,⁴⁶

Submitted to Physical Review D

Work supported in part by DOE Contract No. DE-AC02-76SF00515

S. J. Sekula,⁴⁶ M. Spitznagel,⁴⁶ F. Taylor,⁴⁶ R. K. Yamamoto,⁴⁶ H. Kim,⁴⁷ P. M. Patel,⁴⁷ S. H. Robertson,⁴⁷ A. Lazzaro,⁴⁸ V. Lombardo,⁴⁸ F. Palombo,⁴⁸ J. M. Bauer,⁴⁹ L. Cremaldi,⁴⁹ V. Eschenburg,⁴⁹ R. Godang,⁴⁹ R. Kroeger,⁴⁹ J. Reidy,⁴⁹ D. A. Sanders,⁴⁹ D. J. Summers,⁴⁹ H. W. Zhao,⁴⁹ S. Brunet,⁵⁰ D. Côté,⁵⁰ P. Taras,⁵⁰ F. B. Viaud,⁵⁰ H. Nicholson,⁵¹ N. Cavallo,^{52, †} G. De Nardo,⁵² D. del Re,⁵² F. Fabozzi,^{52, †} C. Gatto,⁵² L. Lista,⁵² D. Monorchio,⁵² P. Paolucci,⁵² D. Piccolo,⁵² C. Sciacca,⁵² M. Baak,⁵³ H. Bulten,⁵³ G. Raven,⁵³ H. L. Snoek,⁵³ C. P. Jessop,⁵⁴ J. M. LoSecco,⁵⁴ T. Allmendinger,⁵⁵ G. Benelli,⁵⁵ K. K. Gan,⁵⁵ K. Honscheid,⁵⁵ D. Hufnagel,⁵⁵ P. D. Jackson,⁵⁵ H. Kagan,⁵⁵ R. Kass,⁵⁵ T. Pulliam,⁵⁵ A. M. Rahimi,⁵⁵ R. Ter-Antonyan,⁵⁵ Q. K. Wong,⁵⁵ N. L. Blount,⁵⁶ J. Brau,⁵⁶ R. Frey,⁵⁶ O. Igonkina,⁵⁶ M. Lu,⁵⁶ C. T. Potter,⁵⁶ R. Rahmat,⁵⁶ N. B. Sinev,⁵⁶ D. Strom,⁵⁶ J. Strube,⁵⁶ E. Torrence,⁵⁶ F. Galeazzi,⁵⁷ A. Gaz,⁵⁷ M. Margoni,⁵⁷ M. Morandin,⁵⁷ A. Pompili,⁵⁷ M. Posocco,⁵⁷ M. Rotondo,⁵⁷ F. Simonetto,⁵⁷ R. Stroili,⁵⁷ C. Voci,⁵⁷ M. Benayoun,⁵⁸ J. Chauveau,⁵⁸ P. David,⁵⁸ L. Del Buono,⁵⁸ Ch. de la Vaissière,⁵⁸ O. Hamon,⁵⁸ B. L. Hartfiel,⁵⁸ M. J. J. John,⁵⁸ J. Malclès,⁵⁸ J. Ocariz,⁵⁸ L. Roos,⁵⁸ G. Therin,⁵⁸ P. K. Behera,⁵⁹ L. Gladney,⁵⁹ J. Panetta,⁵⁹ M. Biasini,⁶⁰ R. Covarelli,⁶⁰ M. Pioppi,⁶⁰ C. Angelini,⁶¹ G. Batignani,⁶¹ S. Bettarini,⁶¹ F. Bucci,⁶¹ G. Calderini,⁶¹ M. Carpinelli,⁶¹ R. Cenci,⁶¹ F. Forti,⁶¹ M. A. Giorgi,⁶¹ A. Lusiani,⁶¹ G. Marchiori,⁶¹ M. A. Mazur,⁶¹ M. Morganti,⁶¹ N. Neri,⁶¹ G. Rizzo,⁶¹ J. Walsh,⁶¹ M. Haire,⁶² D. Judd,⁶² D. E. Wagoner,⁶² J. Biesiada,⁶³ N. Danielson,⁶³ P. Elmer,⁶³ Y. P. Lau,⁶³ C. Lu,⁶³ J. Olsen,⁶³ A. J. S. Smith,⁶³ A. V. Telnov,⁶³ F. Bellini,⁶⁴ G. Cavoto,⁶⁴ A. D’Orazio,⁶⁴ E. Di Marco,⁶⁴ R. Faccini,⁶⁴ F. Ferrarotto,⁶⁴ F. Ferroni,⁶⁴ M. Gaspero,⁶⁴ L. Li Gioi,⁶⁴ M. A. Mazzoni,⁶⁴ S. Morganti,⁶⁴ G. Piredda,⁶⁴ F. Polci,⁶⁴ F. Safai Tehrani,⁶⁴ C. Voena,⁶⁴ M. Ebert,⁶⁵ H. Schröder,⁶⁵ R. Waldi,⁶⁵ T. Adye,⁶⁶ N. De Groot,⁶⁶ B. Franek,⁶⁶ E. O. Olaiya,⁶⁶ F. F. Wilson,⁶⁶ S. Emery,⁶⁷ A. Gaidot,⁶⁷ S. F. Ganzhur,⁶⁷ G. Hamel de Monchenault,⁶⁷ W. Kozanecki,⁶⁷ M. Legendre,⁶⁷ G. Vasseur,⁶⁷ Ch. Yèche,⁶⁷ M. Zito,⁶⁷ W. Park,⁶⁸ M. V. Purohit,⁶⁸ J. R. Wilson,⁶⁸ M. T. Allen,⁶⁹ D. Aston,⁶⁹ R. Bartoldus,⁶⁹ P. Bechtle,⁶⁹ N. Berger,⁶⁹ A. M. Boyarski,⁶⁹ R. Claus,⁶⁹ J. P. Coleman,⁶⁹ M. R. Convery,⁶⁹ M. Cristinziani,⁶⁹ J. C. Dingfelder,⁶⁹ D. Dong,⁶⁹ J. Dorfan,⁶⁹ G. P. Dubois-Felsmann,⁶⁹ D. Dujmic,⁶⁹ W. Dunwoodie,⁶⁹ R. C. Field,⁶⁹ T. Glanzman,⁶⁹ S. J. Gowdy,⁶⁹ M. T. Graham,⁶⁹ V. Halys,⁶⁹ C. Hast,⁶⁹ T. Hryn’ova,⁶⁹ W. R. Innes,⁶⁹ M. H. Kelsey,⁶⁹ P. Kim,⁶⁹ M. L. Kocian,⁶⁹ D. W. G. S. Leith,⁶⁹ S. Li,⁶⁹ J. Libby,⁶⁹ S. Luitz,⁶⁹ V. Luth,⁶⁹ H. L. Lynch,⁶⁹ D. B. MacFarlane,⁶⁹ H. Marsiske,⁶⁹ R. Messner,⁶⁹ D. R. Muller,⁶⁹ C. P. O’Grady,⁶⁹ V. E. Ozcan,⁶⁹ M. Perl,⁶⁹ A. Perazzo,⁶⁹ B. N. Ratcliff,⁶⁹ A. Roodman,⁶⁹ A. A. Salnikov,⁶⁹ R. H. Schindler,⁶⁹ J. Schwiening,⁶⁹ A. Snyder,⁶⁹ J. Stelzer,⁶⁹ D. Su,⁶⁹ M. K. Sullivan,⁶⁹ K. Suzuki,⁶⁹ S. K. Swain,⁶⁹ J. M. Thompson,⁶⁹ J. Va’vra,⁶⁹ N. van Bakel,⁶⁹ M. Weaver,⁶⁹ A. J. R. Weinstein,⁶⁹ W. J. Wisniewski,⁶⁹ M. Wittgen,⁶⁹ D. H. Wright,⁶⁹ A. K. Yarritu,⁶⁹ K. Yi,⁶⁹ C. C. Young,⁶⁹ P. R. Burchat,⁷⁰ A. J. Edwards,⁷⁰ S. A. Majewski,⁷⁰ B. A. Petersen,⁷⁰ C. Roat,⁷⁰ L. Wilden,⁷⁰ S. Ahmed,⁷¹ M. S. Alam,⁷¹ R. Bula,⁷¹ J. A. Ernst,⁷¹ V. Jain,⁷¹ B. Pan,⁷¹ M. A. Saeed,⁷¹ F. R. Wappler,⁷¹ S. B. Zain,⁷¹ W. Bugg,⁷² M. Krishnamurthy,⁷² S. M. Spanier,⁷² R. Eckmann,⁷³ J. L. Ritchie,⁷³ A. Satpathy,⁷³ C. J. Schilling,⁷³ R. F. Schwitters,⁷³ J. M. Izen,⁷⁴ I. Kitayama,⁷⁴ X. C. Lou,⁷⁴ S. Ye,⁷⁴ F. Bianchi,⁷⁵ F. Gallo,⁷⁵ D. Gamba,⁷⁵ M. Bomben,⁷⁶ L. Bosisio,⁷⁶ C. Cartaro,⁷⁶ F. Cossutti,⁷⁶ G. Della Ricca,⁷⁶ S. Dittongo,⁷⁶ S. Grancagnolo,⁷⁶ L. Lancieri,⁷⁶ L. Vitale,⁷⁶ V. Azzolini,⁷⁷ F. Martinez-Vidal,⁷⁷ Sw. Banerjee,⁷⁸ B. Bhuyan,⁷⁸ C. M. Brown,⁷⁸ D. Fortin,⁷⁸ K. Hamano,⁷⁸ R. Kowalewski,⁷⁸ I. M. Nugent,⁷⁸ J. M. Roney,⁷⁸ R. J. Sobie,⁷⁸ J. J. Back,⁷⁹ P. F. Harrison,⁷⁹ T. E. Latham,⁷⁹ G. B. Mohanty,⁷⁹ M. Pappagallo,⁷⁹ H. R. Band,⁸⁰ X. Chen,⁸⁰ B. Cheng,⁸⁰ S. Dasu,⁸⁰ M. Datta,⁸⁰ A. M. Eichenbaum,⁸⁰ K. T. Flood,⁸⁰ J. J. Hollar,⁸⁰ P. E. Kutter,⁸⁰ H. Li,⁸⁰ R. Liu,⁸⁰ B. Mellado,⁸⁰ A. Mihalys,⁸⁰ A. K. Mohapatra,⁸⁰ Y. Pan,⁸⁰ M. Pierini,⁸⁰ R. Prepost,⁸⁰ P. Tan,⁸⁰ S. L. Wu,⁸⁰ Z. Yu,⁸⁰ and H. Neal⁸¹

(The BABAR Collaboration)

¹Laboratoire de Physique des Particules, F-74941 Annecy-le-Vieux, France

²Universitat de Barcelona, Facultat de Fisica Dept. ECM, E-08028 Barcelona, Spain

³Università di Bari, Dipartimento di Fisica and INFN, I-70126 Bari, Italy

⁴Institute of High Energy Physics, Beijing 100039, China

⁵University of Bergen, Institute of Physics, N-5007 Bergen, Norway

⁶Lawrence Berkeley National Laboratory and University of California, Berkeley, California 94720, USA

⁷University of Birmingham, Birmingham, B15 2TT, United Kingdom

⁸Ruhr Universität Bochum, Institut für Experimentalphysik 1, D-44780 Bochum, Germany

⁹University of Bristol, Bristol BS8 1TL, United Kingdom

¹⁰University of British Columbia, Vancouver, British Columbia, Canada V6T 1Z1

¹¹Brunel University, Uxbridge, Middlesex UB8 3PH, United Kingdom

¹²Budker Institute of Nuclear Physics, Novosibirsk 630090, Russia

¹³University of California at Irvine, Irvine, California 92697, USA

¹⁴University of California at Los Angeles, Los Angeles, California 90024, USA

- ¹⁵ University of California at Riverside, Riverside, California 92521, USA
- ¹⁶ University of California at San Diego, La Jolla, California 92093, USA
- ¹⁷ University of California at Santa Barbara, Santa Barbara, California 93106, USA
- ¹⁸ University of California at Santa Cruz, Institute for Particle Physics, Santa Cruz, California 95064, USA
- ¹⁹ California Institute of Technology, Pasadena, California 91125, USA
- ²⁰ University of Cincinnati, Cincinnati, Ohio 45221, USA
- ²¹ University of Colorado, Boulder, Colorado 80309, USA
- ²² Colorado State University, Fort Collins, Colorado 80523, USA
- ²³ Universität Dortmund, Institut für Physik, D-44221 Dortmund, Germany
- ²⁴ Technische Universität Dresden, Institut für Kern- und Teilchenphysik, D-01062 Dresden, Germany
- ²⁵ Ecole Polytechnique, LLR, F-91128 Palaiseau, France
- ²⁶ University of Edinburgh, Edinburgh EH9 3JZ, United Kingdom
- ²⁷ Università di Ferrara, Dipartimento di Fisica and INFN, I-44100 Ferrara, Italy
- ²⁸ Laboratori Nazionali di Frascati dell'INFN, I-00044 Frascati, Italy
- ²⁹ Università di Genova, Dipartimento di Fisica and INFN, I-16146 Genova, Italy
- ³⁰ Harvard University, Cambridge, Massachusetts 02138, USA
- ³¹ Universität Heidelberg, Physikalisches Institut, Philosophenweg 12, D-69120 Heidelberg, Germany
- ³² Imperial College London, London, SW7 2AZ, United Kingdom
- ³³ University of Iowa, Iowa City, Iowa 52242, USA
- ³⁴ Iowa State University, Ames, Iowa 50011-3160, USA
- ³⁵ Johns Hopkins University, Baltimore, Maryland 21218, USA
- ³⁶ Universität Karlsruhe, Institut für Experimentelle Kernphysik, D-76021 Karlsruhe, Germany
- ³⁷ Laboratoire de l'Accélérateur Linéaire, IN2P3-CNRS et Université Paris-Sud 11, Centre Scientifique d'Orsay, B.P. 34, F-91898 ORSAY Cedex, France
- ³⁸ Lawrence Livermore National Laboratory, Livermore, California 94550, USA
- ³⁹ University of Liverpool, Liverpool L69 7ZE, United Kingdom
- ⁴⁰ Queen Mary, University of London, E1 4NS, United Kingdom
- ⁴¹ University of London, Royal Holloway and Bedford New College, Egham, Surrey TW20 0EX, United Kingdom
- ⁴² University of Louisville, Louisville, Kentucky 40292, USA
- ⁴³ University of Manchester, Manchester M13 9PL, United Kingdom
- ⁴⁴ University of Maryland, College Park, Maryland 20742, USA
- ⁴⁵ University of Massachusetts, Amherst, Massachusetts 01003, USA
- ⁴⁶ Massachusetts Institute of Technology, Laboratory for Nuclear Science, Cambridge, Massachusetts 02139, USA
- ⁴⁷ McGill University, Montréal, Québec, Canada H3A 2T8
- ⁴⁸ Università di Milano, Dipartimento di Fisica and INFN, I-20133 Milano, Italy
- ⁴⁹ University of Mississippi, University, Mississippi 38677, USA
- ⁵⁰ Université de Montréal, Physique des Particules, Montréal, Québec, Canada H3C 3J7
- ⁵¹ Mount Holyoke College, South Hadley, Massachusetts 01075, USA
- ⁵² Università di Napoli Federico II, Dipartimento di Scienze Fisiche and INFN, I-80126, Napoli, Italy
- ⁵³ NIKHEF, National Institute for Nuclear Physics and High Energy Physics, NL-1009 DB Amsterdam, The Netherlands
- ⁵⁴ University of Notre Dame, Notre Dame, Indiana 46556, USA
- ⁵⁵ Ohio State University, Columbus, Ohio 43210, USA
- ⁵⁶ University of Oregon, Eugene, Oregon 97403, USA
- ⁵⁷ Università di Padova, Dipartimento di Fisica and INFN, I-35131 Padova, Italy
- ⁵⁸ Universités Paris VI et VII, Laboratoire de Physique Nucléaire et de Hautes Energies, F-75252 Paris, France
- ⁵⁹ University of Pennsylvania, Philadelphia, Pennsylvania 19104, USA
- ⁶⁰ Università di Perugia, Dipartimento di Fisica and INFN, I-06100 Perugia, Italy
- ⁶¹ Università di Pisa, Dipartimento di Fisica, Scuola Normale Superiore and INFN, I-56127 Pisa, Italy
- ⁶² Prairie View A&M University, Prairie View, Texas 77446, USA
- ⁶³ Princeton University, Princeton, New Jersey 08544, USA
- ⁶⁴ Università di Roma La Sapienza, Dipartimento di Fisica and INFN, I-00185 Roma, Italy
- ⁶⁵ Universität Rostock, D-18051 Rostock, Germany
- ⁶⁶ Rutherford Appleton Laboratory, Chilton, Didcot, Oxon, OX11 0QX, United Kingdom
- ⁶⁷ DSM/Dapnia, CEA/Saclay, F-91191 Gif-sur-Yvette, France
- ⁶⁸ University of South Carolina, Columbia, South Carolina 29208, USA
- ⁶⁹ Stanford Linear Accelerator Center, Stanford, California 94309, USA
- ⁷⁰ Stanford University, Stanford, California 94305-4060, USA
- ⁷¹ State University of New York, Albany, New York 12222, USA
- ⁷² University of Tennessee, Knoxville, Tennessee 37996, USA
- ⁷³ University of Texas at Austin, Austin, Texas 78712, USA
- ⁷⁴ University of Texas at Dallas, Richardson, Texas 75083, USA
- ⁷⁵ Università di Torino, Dipartimento di Fisica Sperimentale and INFN, I-10125 Torino, Italy
- ⁷⁶ Università di Trieste, Dipartimento di Fisica and INFN, I-34127 Trieste, Italy
- ⁷⁷ IFIC, Universitat de Valencia-CSIC, E-46071 Valencia, Spain

We describe searches for B meson decays to the charmless vector-vector final states ωK^* , $\omega\rho$, $\omega\omega$, and $\omega\phi$ with 233×10^6 $B\bar{B}$ pairs produced in e^+e^- annihilation at $\sqrt{s} = 10.58$ GeV. We also search for the vector-scalar B decay to ωf_0 . We measure the following branching fractions in units of 10^{-6} : $\mathcal{B}(B^0 \rightarrow \omega K^{*0}) = 2.4 \pm 1.1 \pm 0.7$ (< 4.2), $\mathcal{B}(B^+ \rightarrow \omega K^{*+}) = 0.6^{+1.4+1.1}_{-1.2-0.9}$ (< 3.4), $\mathcal{B}(B^0 \rightarrow \omega\rho^0) = -0.6 \pm 0.7^{+0.8}_{-0.3}$ (< 1.5), $\mathcal{B}(B^+ \rightarrow \omega\rho^+) = 10.6 \pm 2.1^{+1.6}_{-1.0}$, $\mathcal{B}(B^0 \rightarrow \omega\omega) = 1.8^{+1.3}_{-0.9} \pm 0.4$ (< 4.0), $\mathcal{B}(B^0 \rightarrow \omega\phi) = 0.1 \pm 0.5 \pm 0.1$ (< 1.2), and $\mathcal{B}(B^0 \rightarrow \omega f_0) = 0.9 \pm 0.4^{+0.2}_{-0.1}$ (< 1.5). In each case the first error quoted is statistical, the second systematic, and the upper limits are defined at the 90% confidence level. For $B^+ \rightarrow \omega\rho^+$ decays we also measure the longitudinal spin component $f_L = 0.82 \pm 0.11 \pm 0.02$ and the charge asymmetry $\mathcal{A}_{CP} = 0.04 \pm 0.18 \pm 0.02$.

PACS numbers: 13.25.Hw, 12.15.Hh, 11.30.Er

Until recently, hadronic decays of B mesons to pairs of light vector mesons (VV final states) have received less theoretical and experimental attention than decays to two pseudoscalar mesons (PP) or one pseudoscalar and one vector meson (PV). Early papers presented calculations for branching fractions, CP -violating asymmetries [1], and relative spin component contributions [2] for these decays. The measurement three years ago of an unexpectedly small value of the fraction of the longitudinal spin component (f_L) in penguin-dominated $B \rightarrow \phi K^*$ decays [3, 4] triggered new theoretical activity. There have been several attempts to understand the small value of f_L within the Standard Model (SM) [5] and many papers suggested non-SM explanations [6]. Further information about these effects can come from both branching fraction and f_L measurements in decays such as $B \rightarrow \omega K^*$ or $B \rightarrow \omega\phi$, which are conjugate to $B \rightarrow \phi K^*$ via an SU(3) rotation [7]. Information on these and related charmless decays can additionally be used to provide sensitivity to the CKM angles α and γ [8].

We have discussed above mostly penguin-dominated decays. There are also decays with the K^* replaced by a ρ , ω or ϕ meson where tree diagrams are expected to be more important. These include B decays to the final states $\rho\rho$, $\omega\rho$, and $\omega\omega$. The decay $B \rightarrow \rho\rho$ is known to be nearly fully longitudinally polarized [9, 10] and these other predominantly tree decays are expected to behave similarly [11], with branching fractions as predicted in [1].

We report results of measurements of B decays to the charmless VV final states ωV , where V represents a neutral or charged K^* or ρ , or an ω or ϕ meson. We also measure the decay $B^0 \rightarrow \omega f_0(980)$ which shares the same final state as the $B^0 \rightarrow \omega\rho^0$ decay. Due to the current small signal samples, only the branching fractions and the fraction of the longitudinal spin component are measured, the latter by integrating over the azimuthal angles, for which the azimuthal acceptance is uniform. The an-

gular distribution is

$$\frac{1}{\Gamma} \frac{d^2\Gamma}{d\cos\theta_1 d\cos\theta_2} = \frac{9}{4} \left\{ \frac{1}{4}(1 - f_L) \sin^2\theta_1 \sin^2\theta_2 + f_L \cos^2\theta_1 \cos^2\theta_2 \right\}, \quad (1)$$

where θ_k is the helicity angle in the V_k rest frame with respect to the boost axis from the B rest frame and f_L is the fraction of the longitudinal spin component. For $B^+ \rightarrow \omega\rho^+$, we also measure the direct CP -violating time-integrated charge asymmetry $\mathcal{A}_{CP} = (\Gamma^- - \Gamma^+)/(\Gamma^- + \Gamma^+)$, where the superscript on the Γ corresponds to the sign of the B^\pm meson.

The results presented here are based on data collected with the *BABAR* detector [12] at the PEP-II asymmetric e^+e^- collider located at the Stanford Linear Accelerator Center. An integrated luminosity of 211 fb^{-1} , corresponding to 232.8×10^6 $B\bar{B}$ pairs, was recorded at the $\Upsilon(4S)$ resonance (center-of-mass energy $\sqrt{s} = 10.58$ GeV).

Charged particles from the e^+e^- interactions are detected, and their momenta measured, by five layers of double-sided silicon microstrip detectors surrounded by a 40-layer drift chamber, both operating in the 1.5-T magnetic field of a superconducting solenoid. We identify photons and electrons using a CsI(Tl) electromagnetic calorimeter (EMC). Further charged particle identification (PID) is provided by the average energy loss (dE/dx) in the tracking devices and by an internally reflecting ring-imaging Cherenkov detector (DIRC) covering the central region.

We reconstruct the B -daughter candidates through their decays $\rho^0 \rightarrow \pi^+\pi^-$, $f_0(980) \rightarrow \pi^+\pi^-$, $\rho^+ \rightarrow \pi^+\pi^0$, $K^{*0} \rightarrow K^+\pi^-$ (denoted $K_{K^+\pi^-}^{*0}$), $K^{*+} \rightarrow K^+\pi^0$ ($K_{K^+\pi^0}^{*+}$), $K^{*+} \rightarrow K_S^0\pi^+$ ($K_{K_S^0\pi^+}^{*+}$), $\omega \rightarrow \pi^+\pi^-\pi^0$, $\phi \rightarrow K^+K^-$, $\pi^0 \rightarrow \gamma\gamma$, and $K_S^0 \rightarrow \pi^+\pi^-$ (charge-conjugate decay modes are implied throughout). Table I lists the requirements on the invariant mass of these particles' final states. For the ρ , K^* , ϕ , and ω invari-

TABLE I: Selection requirements on the invariant mass and helicity angle of B -daughter resonances. The helicity angle is unrestricted unless indicated otherwise.

State	inv. mass (MeV)	helicity angle
$K_{K^+\pi^-}^{*0}, K_{K_S^0\pi^+}^{*+}$	$755 < m_{K\pi} < 1035$	$-0.85 < \cos \theta < 1.0$
$K_{K^+\pi^0}^{*+}$	$755 < m_{K\pi} < 1035$	$-0.8 < \cos \theta < 1.0$
ρ^0/f_0	$540 < m_{\pi\pi} < 1060$	$-0.85 < \cos \theta < 0.85$
ρ^+	$470 < m_{\pi\pi} < 1070$	$-0.7 < \cos \theta < 0.85$
ω	$740 < m_{\pi\pi\pi} < 820$	
ϕ	$1009 < m_{KK} < 1029$	
π^0	$120 < m_{\gamma\gamma} < 150$	
K_S^0	$473 < m_{\pi\pi} < 522$	

ant masses these requirements are set loose enough to include sidebands, as these mass values are treated as observables in the maximum-likelihood fit described below. The ρ^0 and f_0 (we use f_0 as shorthand for $f_0(980)$) yields are extracted from a simultaneous fit to the same data sample. For K_S^0 candidates we further require the three-dimensional flight distance from the event primary vertex to be greater than three times its uncertainty. Secondary pion and kaon candidates in ρ , K^* , and ω candidates are rejected if their DIRC, dE/dx , and EMC PID signature satisfies tight consistency with protons or electrons, and the kaons (pions) must (must not) have a kaon signature.

Table I also gives the restrictions on the K^* and ρ helicity angles θ (previously defined for Eq. 1), imposed to avoid regions of rapid acceptance variation or combinatorial background from soft particles. To calculate θ we take the angle relative to, for ω , the helicity axis of the normal to the decay plane, for ρ and ϕ , the positively-charged (or only charged) daughter momentum, and for K^* the daughter kaon momentum.

A B -meson candidate is characterized kinematically by the energy-substituted mass $m_{\text{ES}} = \sqrt{(\frac{1}{2}s + \mathbf{p}_0 \cdot \mathbf{p}_B)^2 / E_0^{*2} - \mathbf{p}_B^2}$ and the energy difference $\Delta E = E_B^* - \frac{1}{2}\sqrt{s}$, where (E_0, \mathbf{p}_0) and (E_B, \mathbf{p}_B) are four-momenta of the $\Upsilon(4S)$ and the B candidate, respectively, s is the square of the center of mass energy, and the asterisk denotes the $\Upsilon(4S)$ frame. The resolution on ΔE (m_{ES}) is about 30 MeV (3.0 MeV). Our signal falls in the region $|\Delta E| \leq 0.1$ GeV and $5.27 \leq m_{\text{ES}} \leq 5.29$ GeV, which is then extended to include sidebands that provide a good description of the background. The average number of candidates found per selected event in data is in the range 1.1 to 1.7, depending on the final state. We choose the candidate with the smallest value of a χ^2 constructed from the deviations of the B daughter resonance masses (all particles in Table I except π^0 , K_S^0 , and f_0) from their expected [13] values.

Backgrounds arise primarily from random combinations of particles in continuum $e^+e^- \rightarrow q\bar{q}$ events ($q =$

u, d, s, c). We reduce these by using the angle θ_{T} between the thrust axis of the B candidate in the $\Upsilon(4S)$ frame and that of the rest of the charged and neutral particles in the event. The distribution of $|\cos \theta_{\text{T}}|$ is sharply peaked near 1.0 for $q\bar{q}$ jet pairs, and nearly uniform for B meson decays. The requirements, chosen to reduce the sample size for the large background modes, are $|\cos \theta_{\text{T}}| < 0.9$ for the $\omega\phi$ mode, $|\cos \theta_{\text{T}}| < 0.8$ for the $\omega\omega$ and ωK^* modes, and $|\cos \theta_{\text{T}}| < 0.7$ for the $\omega\rho$ modes. In the maximum-likelihood fit described below, we also use a Fisher discriminant \mathcal{F} that combines four variables defined in the $\Upsilon(4S)$ frame: the polar angles with respect to the beam axis of the B momentum and B thrust axis, and the zeroth and second angular moments, L_0 and L_2 , of the energy flow about the B thrust axis in the $\Upsilon(4S)$ frame. The moments are defined by $L_j = \sum_i p_i \times |\cos \theta_i|^j$, where θ_i is the angle with respect to the B thrust axis of a charged or neutral particle i , p_i is its momentum, and the sum excludes the B candidate's daughters.

From Monte Carlo (MC) simulation [14] we determine the most important charmless $B\bar{B}$ backgrounds (typically about a dozen background modes for each signal final state). We include a variable yield for these in the fit described below. We also introduce a component for non-resonant $\pi\pi$ and $K\pi$ background. The magnitude of this component is fixed in the fit as determined from extrapolations from higher-mass regions.

We obtain yields and values of f_L and \mathcal{A}_{CP} from extended unbinned maximum-likelihood fits with input observables ΔE , m_{ES} , \mathcal{F} and, for the vector meson k , the mass m_k and helicity angle θ_k . For each event i and hypothesis j (signal, $q\bar{q}$ background, $B\bar{B}$ background) we define the probability density function (PDF)

$$\mathcal{P}_j^i = \mathcal{P}_j(m_{\text{ES}}^i) \mathcal{P}_j(\Delta E^i) \mathcal{P}_j(\mathcal{F}^i) \mathcal{P}_j(m_1^i, m_2^i, \theta_1^i, \theta_2^i). \quad (2)$$

We check for correlations in the background observables beyond those accounted for in this PDF and find them to be small. For the signal component, we correct for the effect of small neglected correlations (see below). The likelihood function is

$$\mathcal{L} = \frac{e^{-(\sum Y_j)}}{N!} \prod_{i=1}^N \sum_j Y_j \mathcal{P}_j^i, \quad (3)$$

where Y_j is the yield of events of hypothesis j and N is the number of events in the sample.

The PDF factor for the resonances in the signal takes the form $\mathcal{P}_{1,\text{sig}}(m_1^i) \mathcal{P}_{2,\text{sig}}(m_2^i) \mathcal{Q}(\theta_1^i, \theta_2^i)$ with \mathcal{Q} given by Eq. 1 modified to account for detector acceptance. For $q\bar{q}$ background it is given for each resonance independently by $\mathcal{P}_{q\bar{q}}(m_k^i, \theta_k^i) = \mathcal{P}_{\text{pk}}(m_k^i) \mathcal{P}_{\text{pk}}(\theta_k^i) + \mathcal{P}_{\text{c}}(m_k^i) \mathcal{P}_{\text{c}}(\theta_k^i)$, distinguishing between true resonance (\mathcal{P}_{pk}) and combinatorial (\mathcal{P}_{c}) components. For the $B\bar{B}$ background we assume that all four mass and helicity angle observables are independent.

TABLE II: Signal yield Y and its statistical uncertainty, bias Y_0 , detection efficiency ϵ , daughter branching fraction product $\prod \mathcal{B}_i$, significance S (with systematic uncertainties included), measured branching fraction \mathcal{B} , 90% C.L. upper limit, measured or assumed longitudinal polarization, and \mathcal{A}_{CP} .

Mode	Y (events)	Y_0 (events)	ϵ (%)	$\prod \mathcal{B}_i$ (%)	S (σ)	\mathcal{B} (10^{-6})	\mathcal{B} U.L. (10^{-6})	f_L	\mathcal{A}_{CP}
ωK^{*0}	55_{-19}^{+20}	11	13.2	59.2	2.4	$2.4 \pm 1.1 \pm 0.7$	4.2	$0.71_{-0.24}^{+0.27}$	—
$\omega K_{K^0 \pi^+}^{*+}$	-3.6_{-8}^{+10}	-5	12.5	20.3	0.1	$0.2_{-1.5}^{+1.7} \text{ }_{-1.1}^{+1.5}$	4.2	0.7 fixed	—
$\omega K_{K^+ \pi^0}^{*+}$	12_{-12}^{+14}	6	8.0	29.6	0.5	$1.1_{-2.1}^{+2.5} \text{ }_{-1.2}^{+1.3}$	5.7	0.7 fixed	—
ωK^{*+}					0.4	$0.6_{-1.2}^{+1.4} \text{ }_{-0.9}^{+1.1}$	3.4	0.7 fixed	—
$\omega \rho^0$	-18_{-14}^{+17}	-2	11.6	89.1	0.6	$-0.6 \pm 0.7_{-0.3}^{+0.8}$	1.5	0.9 fixed	—
ωf_0	25_{-11}^{+12}	4	15.2	59.4	2.8	$0.9 \pm 0.4_{-0.1}^{+0.2}$	1.5	—	—
$\omega \rho^+$	156_{-31}^{+33}	11	6.6	89.1	5.7	$10.6 \pm 2.1_{-1.0}^{+1.6}$	—	$0.82 \pm 0.11 \pm 0.02$	$0.04 \pm 0.18 \pm 0.02$
$\omega \omega$	48_{-19}^{+24}	8	12.9	77.5	2.1	$1.8_{-0.9}^{+1.3} \pm 0.4$	4.0	0.79 ± 0.34	—
$\omega \phi$	$3.1_{-8.5}^{+4.4}$	1	19.0	43.2	0.3	$0.1 \pm 0.5 \pm 0.1$	1.2	0.88 fixed	—

For the signal, $B\bar{B}$ background, and non-resonant background components we determine the PDF parameters from simulation. We study large control samples of $B \rightarrow D\pi$ decays of similar topology to verify the simulated resolutions in ΔE and m_{ES} , adjusting the PDFs to account for any differences found. For the continuum background we use $(m_{ES}, \Delta E)$ sideband data to obtain initial values, before applying the fit to data in the signal region, and leave them free to vary in the final fit.

The parameters that are allowed to vary in the fit include the signal, $B\bar{B}$ background, and non-resonant background yields, and continuum background PDF parameters. For the three modes with signals of more than 2σ significance, we vary f_L in the fit to properly account for the variation of efficiency with f_L . For $B^+ \rightarrow \omega \rho^+$ we also vary the signal and background charge asymmetries. For the fits with little signal, we fix f_L to a value that is consistent with *a priori* expectations (see Table II), and account for the associated systematic uncertainty.

To describe the PDFs, we use the sum of two Gaussians for $\mathcal{P}_{sig}(m_{ES})$, $\mathcal{P}_{sig}(\Delta E)$, and the true resonance components of $\mathcal{P}_j(m_k)$; for \mathcal{F} we use an asymmetric Gaussian for signal with a small Gaussian component for background to account for important tails in the signal region. The background m_{ES} shape is described by the function $x\sqrt{1-x^2} \exp[-\xi(1-x^2)]$ (with $x \equiv m_{ES}/E_B^*$) and the distributions of masses m_k by second or third order polynomials. The background PDF parameters that are allowed to vary in the fit are ξ for m_{ES} , slope for ΔE , the polynomial describing the combinatorial component for m_k , and the peak position and lower and upper width parameters for \mathcal{F} .

We evaluate possible biases from our neglect of correlations among discriminating variables in the PDFs by fitting ensembles of simulated experiments into which we have embedded the expected number of signal events and $B\bar{B}$ background events, randomly extracted from the fully-simulated MC samples. We give in Table II the

yield bias Y_0 found for each mode. Since events from a weighted mixture of simulated $B\bar{B}$ background decays are included, the bias we measure includes the effect of this background.

The systematic uncertainties on the branching fractions arising from lack of knowledge of the PDFs have been included in part in the statistical error since most background parameters are free in the fit. For the signal, the uncertainties in PDF parameters are estimated from the consistency of fits to MC and data in large control samples of topology similar to signal. Varying the signal PDF parameters within these errors, we estimate yield uncertainties for each mode. The uncertainty in the yield bias correction is taken to be the quadratic sum of two terms: half the bias correction and the statistical uncertainty on the bias itself. Similarly, we estimate the uncertainty from modeling of the $B\bar{B}$ backgrounds as the change in the signal yield when the number of fitted $B\bar{B}$ events is fixed to be within one sigma of the expected number of $B\bar{B}$ events from MC. For the non-resonant $\pi\pi$ or $K\pi$ backgrounds the uncertainty is taken as the change in the signal when the background yield is varied within the uncertainty of the fits to the higher-mass regions. For modes with fixed f_L , the uncertainty due to the dependence of signal efficiency on f_L is evaluated as the measured change in branching fraction when f_L is varied by ± 0.3 (up to a maximum of $f_L = 1$). These additive systematic errors are dominant for all modes; the PDF variation is always the smallest but the others are typically similar in size.

Uncertainties in our knowledge of the efficiency, found from studies of data control samples, include $0.8\% \times N_t$, $3.0\% \times N_{\pi^0}$, and 1% for a K_S^0 decay, where N_t is the number of tracks, and N_{π^0} is the number of π^0 s in a decay. We estimate the uncertainty in the number of B mesons to be 1.1%. Published data [13] provide the uncertainties in the B -daughter product branching fractions (1–2%). The uncertainties from the event selection are 1–2% for

the requirement on $\cos\theta_T$.

The systematic uncertainty on f_L for $B^+ \rightarrow \omega\rho^+$ includes the effects of fit bias, PDF-parameter variation, and $B\bar{B}$ and non-resonant backgrounds, all estimated with the same method as for the yield uncertainties described above. From large inclusive kaon and B -decay samples, we find a systematic uncertainty for \mathcal{A}_{CP} of 0.02 due mainly to the dependence of reconstruction efficiency on the momentum of the charged ρ daughter. We find for the $B^+ \rightarrow \omega\rho^+$ background, $\mathcal{A}_{CP}^{qq} = -0.010 \pm 0.007$, confirming this estimate.

In Table II we also show for each decay mode the measured branching fraction with its uncertainty and significance together with the quantities entering into these computations. The significance is taken as the square root of the difference between the value of $-2\ln\mathcal{L}$ (with systematic uncertainties included) for zero signal and the value at its minimum. For all modes except for $B^+ \rightarrow \omega\rho^+$ we quote a 90% confidence level (C.L.) upper limit, taken to be the branching fraction below which lies 90% of the total of the likelihood integral in the positive branching fraction region. In calculating branching fractions we assume that the decay rates of the $\Upsilon(4S)$ to B^+B^- and $B^0\bar{B}^0$ are equal [13]. For decays with K^{*+} , we combine the results from the two K^* decay channels, by adding their values of $-2\ln\mathcal{L}$, taking into account the correlated and uncorrelated systematic errors.

We present in Fig. 1 the data and PDFs projected onto m_{ES} and ΔE , for subsamples enriched with a mode-dependent threshold requirement on the signal likelihood (computed without the PDF associated with the variable plotted) chosen to optimize the significance of signal in the resulting subsample. Fig. 2 gives projections of $\cos\theta$ for the $B^+ \rightarrow \omega\rho^+$ decay.

The branching fraction value \mathcal{B} given in Table II for $B^+ \rightarrow \omega\rho^+$ comes from a direct fit with the free parameters \mathcal{B} and f_L , as well as \mathcal{A}_{CP} . This choice exploits the feature that \mathcal{B} is less correlated with f_L than is either the yield or efficiency taken separately. The behavior of $-2\ln\mathcal{L}(f_L, \mathcal{B})$ is shown in Fig. 3.

In summary, we have searched for seven charmless hadronic B -meson decays. We observe $B^+ \rightarrow \omega\rho^+$ with a significance of 5.7σ , and establish improved 90% C.L. upper limits for the other modes, with the following branching fractions:

$$\begin{aligned} \mathcal{B}(B^0 \rightarrow \omega K^{*0}) &= 2.4 \pm 1.1 \pm 0.7 (< 4.2) \times 10^{-6}, \\ \mathcal{B}(B^+ \rightarrow \omega K^{*+}) &= 0.6_{-1.2}^{+1.4+1.1} (< 3.4) \times 10^{-6}, \\ \mathcal{B}(B^0 \rightarrow \omega\rho^0) &= -0.6 \pm 0.7_{-0.3}^{+0.8} (< 1.5) \times 10^{-6}, \\ \mathcal{B}(B^+ \rightarrow \omega\rho^+) &= 10.6 \pm 2.1_{-1.0}^{+1.6} \times 10^{-6}, \\ \mathcal{B}(B^0 \rightarrow \omega\omega) &= 1.8_{-0.9}^{+1.3} \pm 0.4 (< 4.0) \times 10^{-6}, \\ \mathcal{B}(B^0 \rightarrow \omega\phi) &= 0.1 \pm 0.5 \pm 0.1 (< 1.2) \times 10^{-6}, \text{ and} \\ \mathcal{B}(B^0 \rightarrow \omega f_0) &= 0.9 \pm 0.4_{-0.1}^{+0.2} (< 1.5) \times 10^{-6}. \end{aligned}$$

In each case the first error quoted is statistical, the second

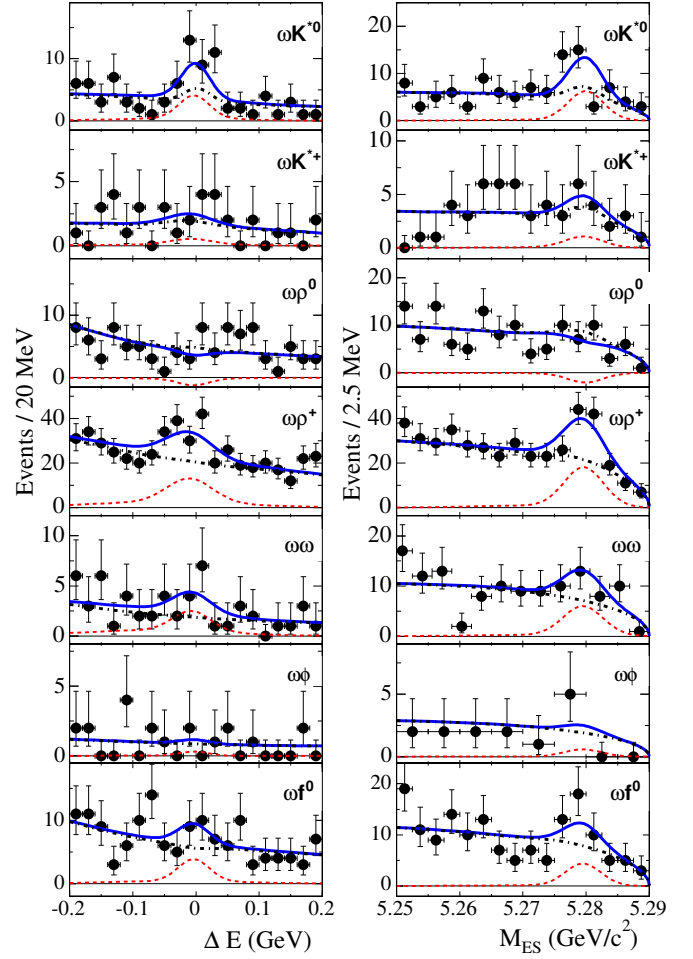


FIG. 1: Projections of ΔE (left) and m_{ES} (right) of events passing a signal likelihood threshold for, from top to bottom, $B^0 \rightarrow \omega K^{*0}$, $B^+ \rightarrow \omega K^{*+}$, $B^0 \rightarrow \omega\rho^0$, $B^+ \rightarrow \omega\rho^+$, $B^0 \rightarrow \omega\omega$, $B^0 \rightarrow \omega\phi$, and $B^0 \rightarrow \omega f_0$. The solid curve is the fit function, the dashed curve is the signal contribution, and the dot-dashed curve is the background contribution.

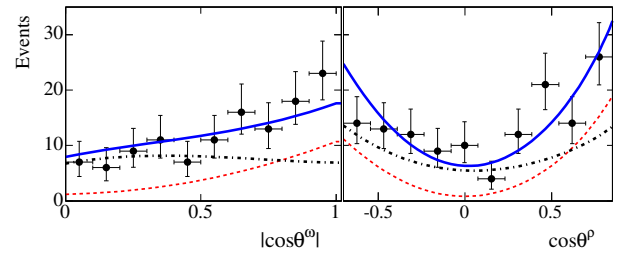


FIG. 2: Projections of helicity-angle cosines, of events passing a signal likelihood threshold for ω (left) and ρ^+ (right) from the fit for $B^+ \rightarrow \omega\rho^+$ decay. The solid curve is the fit function, the dashed curve is the signal contribution, and the dot-dashed curve is the background contribution.

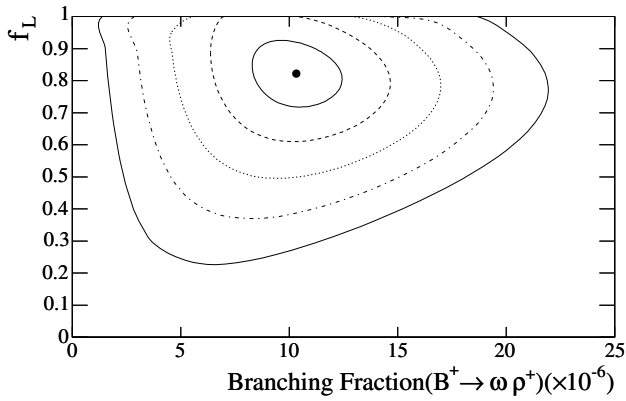


FIG. 3: Distribution of $-2 \ln \mathcal{L}(f_L, \mathcal{B})$ for $B^+ \rightarrow \omega \rho^+$ decay. The solid dot gives the central value; curves give the contours in 1-sigma steps ($\Delta \sqrt{-2 \ln \mathcal{L}(f_L, \mathcal{B})} = 1$).

systematic, and the upper limits are taken at 90% C.L.

For $B^+ \rightarrow \omega \rho^+$ we also measure the longitudinal spin component $f_L = 0.82 \pm 0.11 \pm 0.02$ and charge asymmetry $\mathcal{A}_{CP} = 0.04 \pm 0.18 \pm 0.02$. The longitudinal spin component is dominant, as it is for $B \rightarrow \rho \rho$ [9, 10]. Assuming tree dominance we would naively expect the branching fraction for $B^+ \rightarrow \omega \rho^+$ to be equal to that of $B^+ \rightarrow \rho^+ \rho^0$. However the measured branching fraction for $\mathcal{B}(B^+ \rightarrow \omega \rho^+)$ is more than two standard deviations smaller than the world average $\mathcal{B}(B^+ \rightarrow \rho^+ \rho^0) = 26 \pm 6 \times 10^{-6}$ [13].

Our branching fraction results are in agreement with theoretical estimates [1, 11].

We are grateful for the excellent luminosity and machine conditions provided by our PEP-II colleagues, and for the substantial dedicated effort from the computing organizations that support BABAR. The collaborating institutions wish to thank SLAC for its support and kind hospitality. This work is supported by DOE and NSF (USA), NSERC (Canada), IHEP (China), CEA and CNRS-IN2P3 (France), BMBF and DFG (Germany), INFN (Italy), FOM (The Netherlands), NFR (Norway), MIST (Russia), and PPARC (United Kingdom). Individuals have received support from CONACyT (Mexico), Marie Curie EIF (European Union), the A. P. Sloan Foundation, the Research Corporation, and the Alexander von Humboldt Foundation.

* Also at Laboratoire de Physique Corpusculaire, Clermont-Ferrand, France

† Also with Università di Perugia, Dipartimento di Fisica, Perugia, Italy

‡ Also with Università della Basilicata, Potenza, Italy

- [1] G. Kramer and W.F. Palmer, Phys. Rev. D **45**, 193 (1992); G. Kramer and W.F. Palmer, Phys. Rev. D **46**, 2969 (1992); A. Ali, G. Kramer, and C.-D. Lü, Phys. Rev. D **58**, 094009 (1998); A. Ali, G. Kramer, and C.-D. Lü, Phys. Rev. D **59**, 014005 (1999); Y.H. Chen *et al.*, Phys. Rev. D **60**, 094014 (1999); H. Y. Cheng and K.C. Yang, Phys. Lett. B **511**, 40 (2001).
- [2] G. Kramer and W.F. Palmer, Phys. Lett. B **279**, 181 (1992).
- [3] BABAR Collaboration, B. Aubert *et al.*, Phys. Rev. Lett. **91**, 171802 (2003); BABAR Collaboration, B. Aubert *et al.*, Phys. Rev. Lett. **93**, 231804 (2004).
- [4] Belle Collaboration, K.F. Chen *et al.*, Phys. Rev. Lett. **91**, 201801 (2003); Belle Collaboration, K.F. Chen *et al.*, Phys. Rev. Lett. **94**, 221804 (2005).
- [5] C.W. Bauer *et al.*, Phys. Rev. D **70**, 054015 (2004); P. Colangelo, F. De Fazio and T.N. Pham, Phys. Lett. B **597**, 291 (2004); A.L. Kagan, Phys. Lett. B **601**, 151 (2004); M. Ladisa *et al.*, Phys. Rev. D **70**, 114025 (2004); H. Y. Cheng, C. K. Chua and A. Soni, Phys. Rev. D **71**, 014030 (2005); H.-n. Li and S. Mishima, Phys. Rev. D **71**, 054025 (2005); H.-n. Li, Phys. Lett. B **622**, 63 (2005).
- [6] W. Bensalem and D. London, Phys. Rev. D **64**, 116003 (2001); A. K. Giri and R. Mohanta, Phys. Rev. D **69**, 014008 (2004); E. Alvarez *et al.*, Phys. Rev. D **70**, 115014 (2004); C.-H. Chen and C.-Q. Geng, Phys. Rev. D **71**, 115004 (2005); P. K. Das and K. C. Yang, Phys. Rev. D **71**, 015009 (2005); C.-H. Chen and C.-Q. Geng, Phys. Rev. D **71**, 115004 (2005); Y.-D. Yang, R. M. Wang and G. R. Lu, Phys. Rev. D **72**, 094002 (2005); A. K. Giri and R. Mohanta, Eur. Phys. Jour. C **44**, 249 (2005); S. Baek *et al.*, Phys. Rev. D **72**, 094008 (2005).
- [7] S. Oh, Phys. Rev. D **60**, 034006 (1999).
- [8] D. Atwood and A. Soni, Phys. Rev. D **59**, 013007 (1999); D. Atwood and A. Soni, Phys. Rev. D **65**, 073018 (2002); H.-W. Huang *et al.*, Phys. Rev. D **73**, 014011 (2006).
- [9] BABAR Collaboration, B. Aubert *et al.*, Phys. Rev. Lett. **91**, 171802 (2003); BABAR Collaboration, B. Aubert *et al.*, Phys. Rev. D **69**, 031102 (2004); BABAR Collaboration, B. Aubert *et al.*, Phys. Rev. Lett. **93**, 231801 (2004); BABAR Collaboration, B. Aubert *et al.*, Phys. Rev. Lett. **95**, 041805 (2005).
- [10] Belle Collaboration, J. Zhang *et al.*, Phys. Rev. Lett. **91**, 221801 (2003); Belle Collaboration, A. Somov, A.J. Schwartz *et al.*, hep-ex/0601024 (2006).
- [11] Y. Li and C.-D. Lü, Phys. Rev. D **73**, 014024 (2006).
- [12] BABAR Collaboration, B. Aubert *et al.*, Nucl. Instr. Methods Phys. Res., Sect. A **479**, 1 (2002).
- [13] Particle Data Group, S. Eidelman *et al.*, Phys. Lett. B **592**, 1 (2004).
- [14] The BABAR detector Monte Carlo simulation is based on GEANT4: S. Agostinelli *et al.*, Nucl. Instr. Methods Phys. Res., Sect. A **506**, 250 (2003).